PROCEEDINGS, Thirty-Seventh Workshop on Geothermal Reservoir Engineering
Stanford University, Stanford, California, January 30 - February 1, 2012
SGP-TR-194

THE POTENTIAL OF SHALLOW GROUNDWATER RESOURCES FOR COOLING PURPOSES - A GEOTHERMAL CASE STUDY IN NORTH EAST JORDAN

S. Al-Zyoud, W. Rühaak and I. Sass

Chair of Geothermal Science and Technology, Institute of Applied Geosciences
Schnittspahnstrasse 9, 64287 Darmstadt, Germany
al-zyoud@geo.tu-darmstadt.de; ruehaak@geo.tu-darmstadt.de; sass@geo.tu-darmstadt.de

ABSTRACT

Geothermal energy as a sustainable resource has the potential to significantly contribute to the cooling of buildings in Jordan. A shallow aquifersystem in north east Jordan was proven as a geothermal resource for its potential for cooling utilization. The investigation involved the development of various numerical 3D models in order to predict the future performance of the geothermal reservoir for different possible geothermal installation.

The study showed that a geothermal utilization of the studied basaltic reservoir is feasible. It features sufficient hydraulic and thermal properties to be utilized for cooling purposes. Furthermore the models developed for this reservoir have proven to be robust and flexible. Therefore they can be used with new thermophysical and hydrogeological data to construct and analyze further near surface geothermal resources in Jordan.

INTRODUCTION

Due to climate change the maximum summer temperatures in arid regions as well as in other parts of the world are generally increasing. As a result, the demand for cooling of buildings and industrial facilities is increasing and requires large energy related investments. These increasing cooling demands are mostly served by conventional fossil energy sources.

The utilization of geothermal resources for heating and power generation is well established. However, using the relatively low temperature of the shallow subsurface and of the groundwater for cooling purposes is also a viable geothermal application.

The geothermal installations discussed here in are intended to provide cooling for different types of buildings.

All geothermal cooling installations discussed are open loop systems, consisting of an array of vertical wellbores for cool groundwater extraction and reinjection of the warmed water.

The production horizons discussed in this study is the upper basaltic groundwater reservoir in the Amman Zarqa basin in north east Jordan. A basaltic formation located within the Jordanian Harrat basaltic rocks of north east Jordan; composed of several volcanic flow extrusions with different thicknesses ranging from 50 m to 400 m with an average thickness of 250 m (Ibrahim, 1993). An additional potential target layer, below the basalt flows, is a late cretaceous limestone formation with a thickness of about 250 m (Abu Qudaira, 2004).

The hydraulic and thermophysical characteristics of the Jordanian Harrat basalt were evaluated based on 72 thermal conductivity, permeability and porosity measurements. Also several historic and recent groundwater level measurements were evaluated.

Due to a relatively high porosity and permeability, enhanced by numerous NW-SE and some NE-SW trending faults (see Fig. 1), these formations are an important shallow aquifer. Also the proximity to potential consumers with a demand for cooling applications is favorable.

JORDANIAN HARRAT

Geology

The Jordanian Harrat basalt is part of a large intra-continental flood basalt, extending over the northern Jordanian desert (Fig. 1). They are part of the Cenozoic continental basaltic formation known as Harrat Ash Shaam covering an area of ca. 12.000 km^2 (Al Malabeh, 2011). Together with the underlying limestone, the basalt represents the shallow groundwater aquifer of the Amman Zarqa basin (Al-Kharabsheh & Al-Malabeh, 2002). The underlying limestone formation (Fig. 1 and 2) is a creamy yellowish, massive dolomitic limestone in intercalation with the Coquina limestone (Smadi, 2000) and chert bearing limestones (Abu Qudaira, 2004).

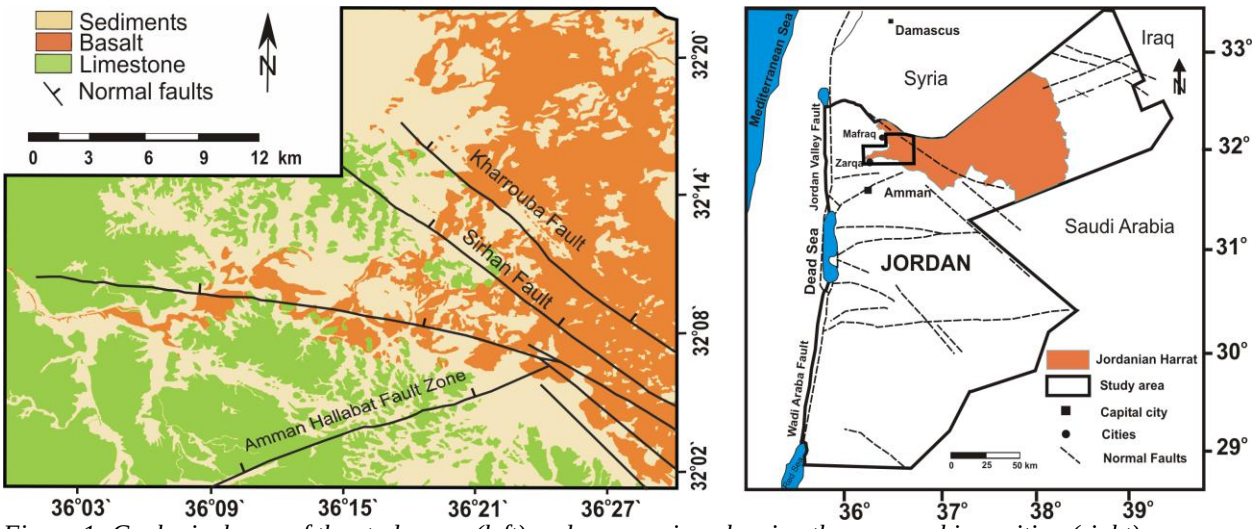

Figure 1: Geological map of the study area (left) and an overview showing the geographic position (right).

Hydrogeology

The main layers of the studied reservoir are represented by the basaltic eruption on top of the fractured limestone succession. Limestones and basalts are hydraulically connected, representing a fractured aquifer (Fig. 2). They are underlain by a 20–35 m thick marl formation. The limestone formation features a great lateral extent in combination with a reasonable hydraulic conductivity. The mean hydraulic conductivity of the limestone, based on pumping tests, is $8.1 \cdot 10^{-5}$ m s^{-1} (Al Mahamid, 2005). The uppermost basaltic aquifer is formed by highly vesicular and fractured lava flows. The mean hydraulic conductivity of the basalts is good and ranges around $4 \cdot 10^{-4}$ m s^{-1}.

In general the water level is declining in almost all wells within the basin. The drawdown is reported by the Ministry of Water and Irrigation (MWI, 2000) to range between 0.67 m and 2.0 m per year all over the basin. According to Al-Zyoud et al. (2012) the groundwater drawdown in the study area is 1.1 m per year.

Thermophysical properties

Several thermophysical parameters were determined (Table 1). Thermal conductivity and permeability are the most important thermophysical rock parameters for locating and developing any geothermal reservoir. Knowledge of thermal conductivity is an absolute necessity for the calculation of heat flow models (Sass et al., 1971). Knowledge of the rock permeability is required for its effective hydraulic conductivity in the geothermal reservoir. In these thermophysical investigations two of a total of six basaltic flows in the Jordanian Harrat were studied. Lithologically both studied basalt flows were subdivided into six subflows, three each. The thermal conductivity and permeability relationship of the basalts was determined (Fig. 3).

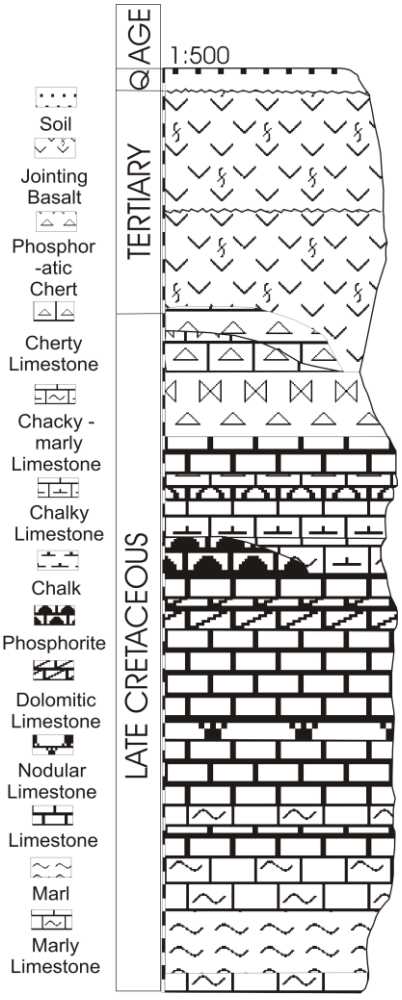

Figure 2: The lithology of the cooling reservoir aquifer system.

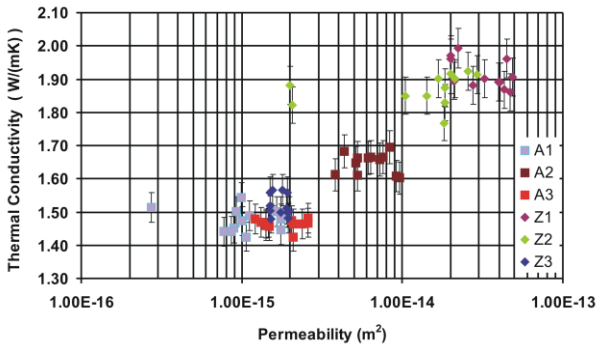

Figure 3: The Thermal conductivity and permeability for Jordanian Harrat basalts. Z1 is the lowest lava flow and A3 is the highest one.

COOLING APPLICATIONS

The three different cooling applications (Table 2) discussed in the following are intended to provide cooling for the Al Hussein Thermal Power Station, Hashemite University and 100 houses as a representative sample from 170,000 homes dispersed in six conurbation areas in the western part of the trap basalts (Fig. 4).

The necessary amount of water for cooling was calculated based on an approximated temperature spread between extraction and injection (Table 2).
The resulting cooling load is calculated according to:

$$Q_m = (\rho c)_f \cdot (T_i - T_o) \cdot q \qquad (1)$$

Where Q_m is the cooling load (W), $(\rho c)_f$ is the volumetric heat capacity of the pumped water (J m^{-3} K^{-1}), T_i is the injection temperature (°C) – a constant boundary condition, T_o is the computed extraction temperature (°C) and q is the flow rate (m^3 s^{-1}), set as 4th kind boundary condition (in FEFLOW® nomenclature).

Each scenario is computed for a time-span of 10 years.

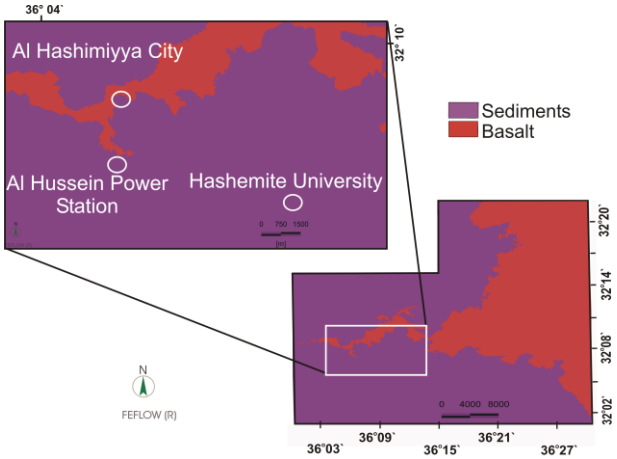

Figure 4: Location of the three scenarios within the model domain.

NUMERICAL MODELING OF DIFFERENT COOLING SCENARIOS

To estimate the applicability and effectiveness of different well array configurations a numerical computation of the long term heat-transport in the subsurface is necessary.

Structural model

Based on the lithological and additional structural geologic data from a borehole database (Ibrahim, 1993; Smadi, 2000; Abu Qudaira, 2004; MWI, 2010), including major faults, a structural 3D model was created with GOCAD® (Mallet, 2002). The model covers an area of about 400 km^2. The generalized geological units are defined in Table 1.

Table 1: Lithology, hydraulic and thermophysical properties of the modeled units.

Unit	Stratigraphic Unit	Predominant Lithology	Thermal Conductivity (Matrix) (W m^{-1} K^{-1})	Specific Heat Capacity (Matrix) (kJ kg^{-1} K^{-1})	Porosity (-)	Density (kg m^{-3})	Hydraulic Conductivity (m s^{-1})
1	Quaternary	Sediments (Silt, Sand & Gravel)	0.58	0.80	0.35	1,420	$5.8 \cdot 10^{-7}$
2	Tertiary	Basalt	1.65	0.86	0.15	2,660	$4.0 \cdot 10^{-4}$
3	Late Cretaceous	Limestone	2.36	0.84	0.10	2,550	$2.0 \cdot 10^{-5}$
4	Late Cretaceous	Marl	2.25	0.84	0.02	2,740	$1.0 \cdot 10^{-9}$

Table 2: Cooling scenarios.

Nr	Scenario	Temperature Difference (K)	Cooling load (MW)	Groundwater discharge (m^3 d^{-1})
(1)	Al Hussein Thermal Power Station	8	0.93	2,400
(2)	Hashemite University	9	3.50	8,000
(3)	Al Hashimiyya - Zarqa City (100 houses)	9	2.20	5,200

Heat transport model

Based on the structural GOCAD® model a FEFLOW® (Diersch, 2005) 3D groundwater flow and heat transport model was created (Fig. 4). The numerical model has the same geometry as the GOCAD® model. The uppermost sedimentary layer exists only in some parts of the model region. However, FEFLOW® slices have to be continuous. To meet this requirement the non-continuous slices are continued with a minimum thickness of 0.1 m while the assigned parameters are according to the underlying unit.

Thermophysical data

The input data are given in Table 1. Most of the values result from measurements performed for this study. Values for marl and limestone were published by Al Mahamid (2005). The resulting bulk values of thermal conductivity and specific heat capacity are calculated as linear average with respect to the porosity, using either the standard properties of water or - in the upper unsaturated part of the model - the respective values for air.

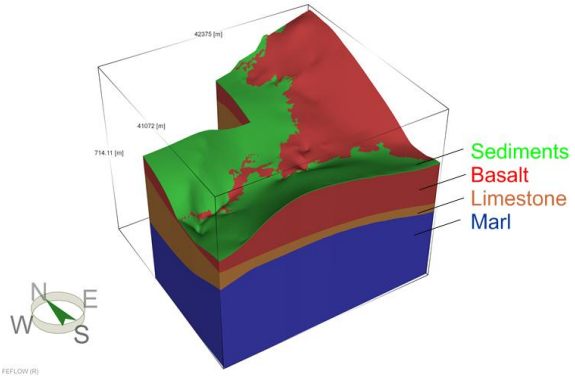

Figure 5: The structural 3D model.

Flow - initial and boundary conditions

The availability of high quality hydrological data is limited (MWI, 2010). The data are extremely fluctuating over time due to the intense but also variable groundwater extraction; mostly for irrigation. Therefore it is difficult to derive a realistic areal groundwater head distribution. Data sets beginning from the year 1965 were evaluated. For this study the data-set of the year 1998 was used as reference data, mainly because for this year the highest number of measurements is available. In a first step the head values were gridded to the model area using the local polynomial filtering and interpolating approach of the software Surfer®. The resulting hydraulic head distribution is used in a FEFLOW® steady state flow model as initial and 1st kind boundary condition of the modeling area. The equilibrium head distribution achieved this way is then used for a transient model. Here, also average values of all known pumping activities are assigned to the specific nodes in the model area. This run was computed for a simulation period of 12 years, ending December 31, 2010.

Eight monitoring wells with continuous records were selected to calibrate the model. The model reflects the above mentioned average drawdown rate of 1.1 m a^{-1} well. To achieve this it was necessary to transform the previous 1st kind boundary conditions to equivalent nodal sources (in FEFLOW® nomenclature "4th kind" boundary condition). The final initial head distribution of the model is shown in Fig. 6.

All modeled cooling scenarios begin on January 1st, 2011 and run for 10 years.

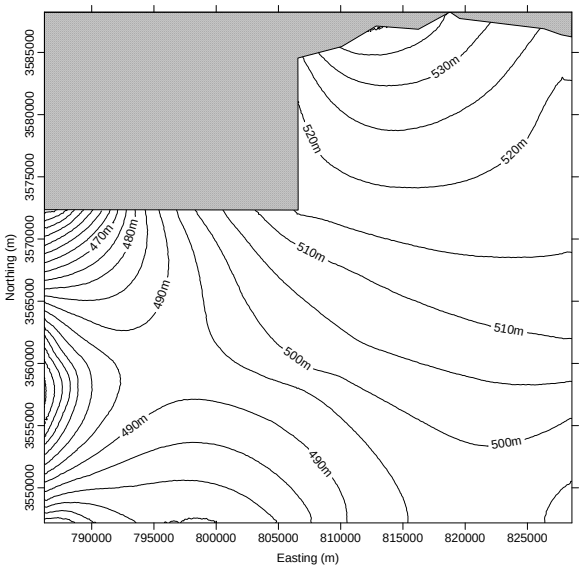

Figure 6: Hydraulic head distribution in the model area, used as initial condition (December 31, 2010) and as boundary condition at the outer margins. (Coordinates are given in UTM).

Heat - initial and boundary conditions

Information about the subsurface temperature distribution in the study area is very limited. Thus, an initial quasi steady state temperature distribution was computed. For this computation a surface temperature of 19 °C was set as 1st kind boundary condition on top of the model and a basal heat flow rate of 100 mW m^{-2} according to the global heat flow data base (Pollack et al., 1993), as 2nd kind boundary condition at the bottom of the model. The thermal conductivity of the subsurface is given in Table 1. To bring this temperature distribution into equilibrium with the pumping activities a transient heat transport model from 1998 till 2010 is computed, starting with the quasi steady state result. The temperature distribution at the end of this run (Fig. 7) is then used

as initial and boundary condition for the scenario runs. In the latter simulations the bottom 2nd kind (Neumann) boundary condition is replaced with an equivalent 1st kind (Dirichlet) boundary condition to improve the stability of the simulation process. A comparison of the resulting temperature profile with measured logs outside the model area (there are no logs with a sufficient depth available inside the model area) shows a good agreement.

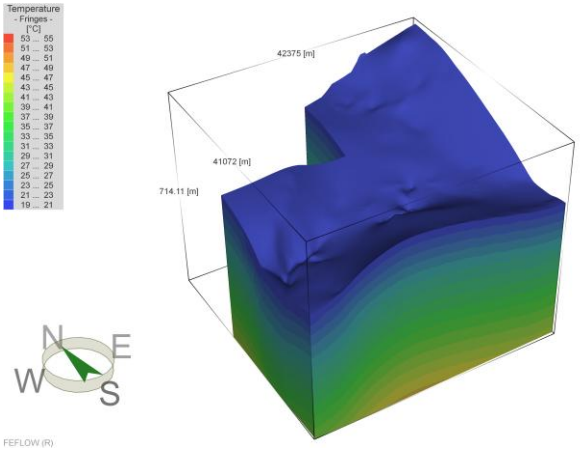

Figure 7: 3D view of the initial temperature distribution

Temperature dependence of the fluid viscosity and density is not taken into account.

The mean daily air temperature in summer is 24 °C and in winter is 17°C. A wide range of air temperature is recorded in this area due to the arid climate. Minimum temperatures in winter can reach 2 °C, while the maximum temperature is typically around 18 °C. In summer the minimum temperature does not fall below 15 °C, while the maximum temperature may reach up to 43 °C.

Setup of the three cooling scenarios

The extraction of the relatively cool groundwater may be achieved by different arrays of extraction wells, see Fig. 8. For the injection wells the same well geometry is applied. For scenario (1), 24 wells with a spacing of 125 m, for scenario (2), 40 wells with a spacing of 35 m and for scenario (3), 26 wells with a spacing of 25 m are used. In scenario (1) 100 $m^3 d^{-1}$ pumping rate for each well is applied. For the other two scenarios the pumping rate is 200 $m^3 d^{-1}$ for each well.

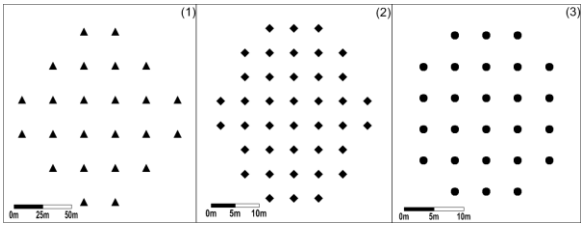

Figure 8: Configuration of the well arrays for the three different cooling scenarios.

For the three scenarios, the groundwater extraction takes place at different depths ((1) 130 m, (2) 90 m, (3) 40 m below ground surface) using multi-level wells. The injection wells reach depths of 50 m below the ground surface. For the simulation of the effect of injecting heated water, a fixed temperature boundary condition of 34 °C, 28 °C, 28 °C is assigned to wells in scenarios (1), (2) and (3), respectively.

The relative positions of extraction and injection wells are shown in Fig. 9. The distance between the arrays is approximately (1) 1300 m, (2) 800 m and (3) 1700 m, respectively.

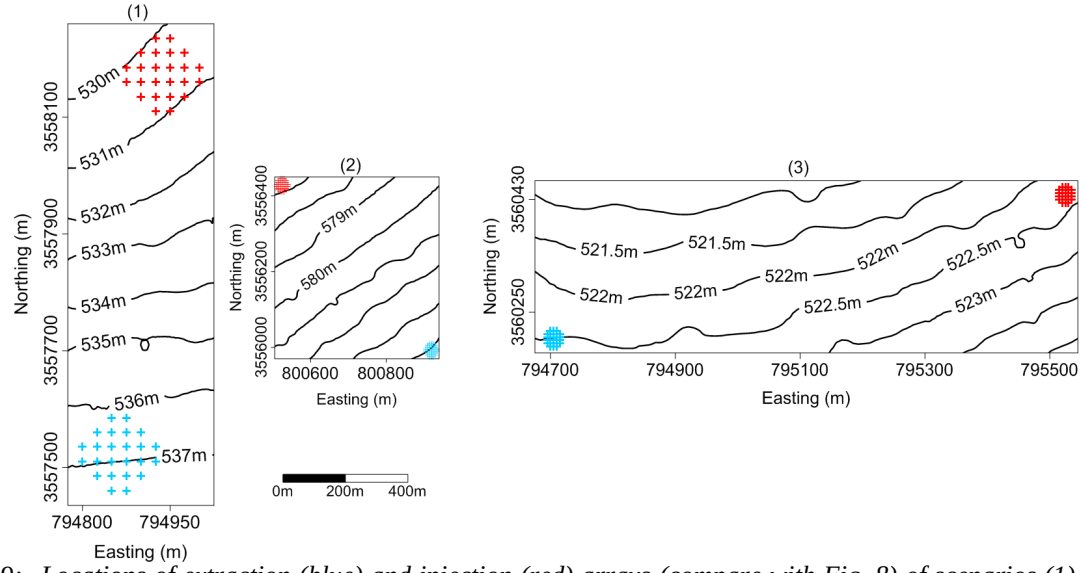

Figure 9: Locations of extraction (blue) and injection (red) arrays (compare with Fig. 8) of scenarios (1), (2) and (3); additionally the groundwater head isolines are given.

RESULTS

Temperature differences between extraction and injection wells were derived from the FEFLOW® simulation model.

The cooling load progression (see Eq. 1) for a 10 year simulation period for the three scenarios is shown in Fig. 10.
In scenario (1) the obtained cooling load of approximately 1 MW slightly increases with time. The available cooling loads of approximately 2.6 MW for scenario (2) and 1.95 MW for scenario (3) decrease with time, after an initial rapid increase.

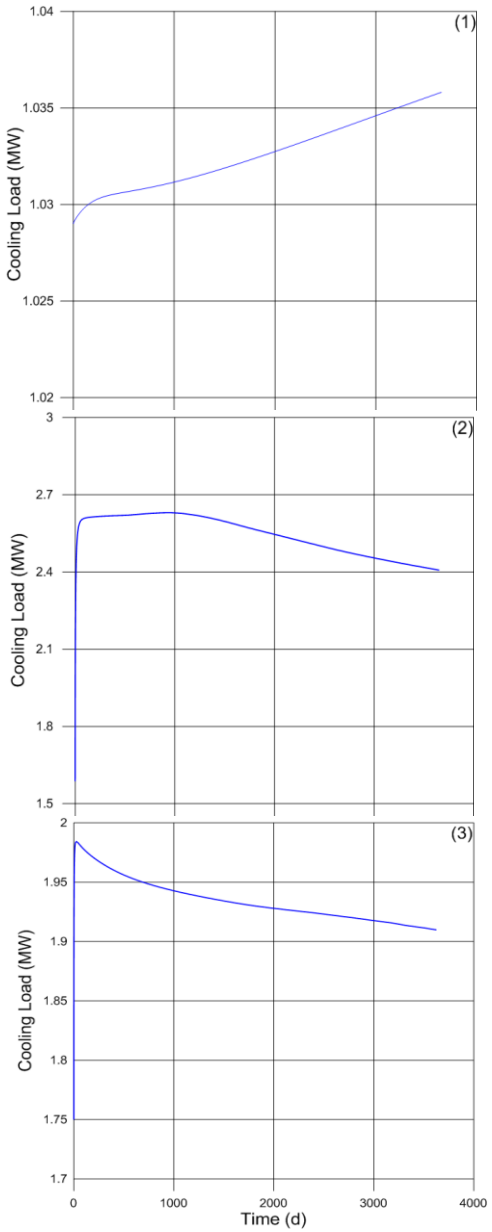

Figure 10: Cooling load for the studied scenarios

Fig. 11 shows the temperatures at the extraction wells. Due to the different locations and therefore differences regarding lithology, groundwater level and hydraulic situation, the results of the modeled cooling load and of the temperature at the extraction wells each show an individual trend. Scenarios (1) and (2) show a decrease of the temperature (approximately 1 K) at a number of extraction wells. This is due to the higher vertical hydraulic conductivity at the locations of scenarios (1) and (2) compared to the vertical hydraulic conductivity at the location of scenario (3). However, based on the hydrologic situation this result is reasonable as slightly cooler water from overlying layers is pumped.

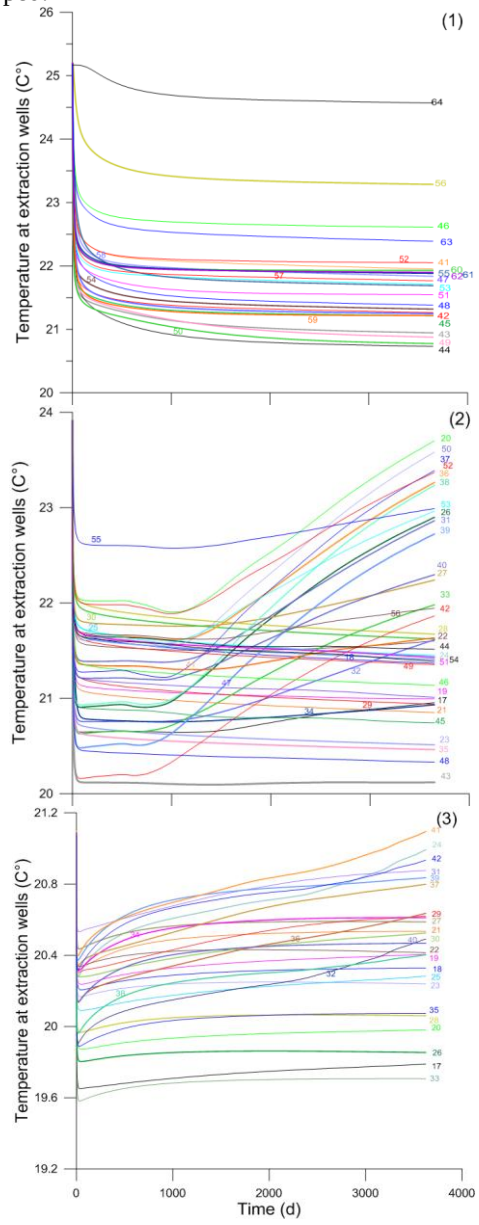

Figure 11: Local temperature distribution for each extraction array.

In scenario (3) the temperature increases because the ground temperature around the array of extraction wells increases with time due to the heat dissipated by reinjected water. This thermal short-circuit is due to the too short distance between extraction and injection well arrays together with the parallel oriented groundwater flow-field. However, the setup was limited due to the existing constructions in the scenario area.

CONCLUSIONS AND OUTLOOK

Despite the relatively high surface temperatures the cooling system approach presented here satisfies the actual cooling load demands in all three cases.
A cooling efficiency for each scenario can be calculated based on:

$$Efficiency = \frac{Q_m}{Q} \cdot 100\% \qquad (2)$$

Where Q_m is the modeled cooling load and Q is the cooling load demand.

The cooling efficiency and the derived potential of the studied scenarios are given in Table 4 and Fig. 12.

Table 4: Calculated cooling system efficiency.

Scenario	Efficiency (%)
(1) Power Station	99.5
(2) Hashemite University	45
(3) Al Hashimiyya City	87

In scenarios (1) and (3) sufficient cooling loads can be achieved. However, there are several realistic options to increase the cooling loads of scenario (2), too. Especially the application of so called night sky cooling (e.g. Dobson, 2005) could increase the overall efficiency substantially. Another option would be to use electric energy (e.g. by photovoltaic) and to couple heat pumps to the system.
Changing the flow direction of the system seasonally in scenario (3) by reversing injection and extraction arrays will increase the efficiency of the cooling system; additionally as it can prevent a thermal short-circuit.
Negative effects on the groundwater due to the warming, e.g. chemical and microbiological, are not discussed here. However, they have to be examined thoroughly before starting such geothermal applications to avoid a negative impact on this most important resource. The ongoing groundwater mining, predominantly for irrigation purposes, may also lead to a conflict with possible energy application in this aquifer system.

ACKNOWLEDGMENTS

The authors thank German Exchange Academic Service (DAAD) and HSE NATURpur Energie AG for financial support.
Warm thanks for Prof. Ahmad Al-Malabeh for his valuable cooperation in the field work and rock sampling.
Sincerely gratitude extended to Dr. Ahmad Al- Ghandoor for his help in cooling load calculations.
Many thanks go to Ministry of Water and Irrigation who very kindly gave us permission to use the available groundwater database.
The first author thanks Technische Universität Darmstadt for financial support by the Frauenfördermittel fund.

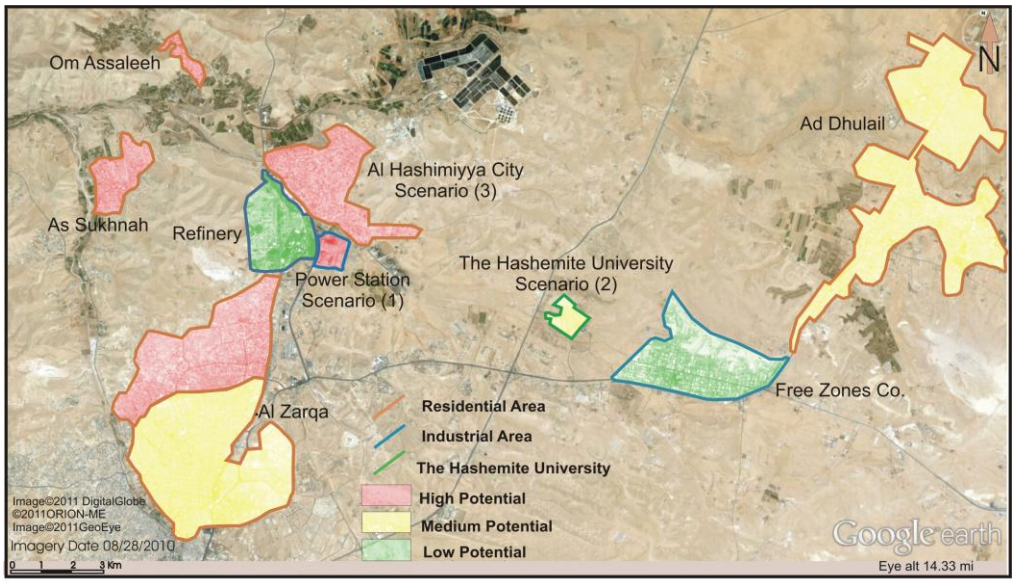

Figure 12: Geothermal cooling potential derived from the results of the numerical modeling (positions are according to Fig. 4).

REFERENCES

Abu Qudaira, M. (2004), "The geology of Zarqa area," *Natural Resources Authority Bulletin*, **58**, 45.

Al Mahamid, J. (2005), "Integration of water resources of the upper aquifer in Amman – Zarqa basin based on mathematical modeling and GIS, Jordan", *Freiberg Online Geology*, **12**, 223.

Al-Kharabsheh A., and Al-Malabeh A. (2002), "Water Harvesting in Wadi Al-Maghyer, Azraq Basin-Jordan and its Environmental Impacts," *Proceeding of Congress in Urban Developments in Arid region & Associated Problems*, **3**, 97-106.

Al-Malabeh, A. (2011), "New subdivision of Jordanian Harrat: A spatial and temporal distribution and their source regions," *Earth Science and Engineering*, **1** (in press)

Al-Zyoud, S, Rühaak, W. and Sass, I. (2012), "Over exploitation of Groundwater in the Centre of Amman Zarqa Basin – Jordan," *Ground Water Monitoring & Remediation*. (Submitted)

Diersch, H.-J.G. (2005), "FEFLOW finite element subsurface flow and transport simulation system," *reference manual, WASY, Institute for Water Resources Planning and Systems Research*, Berlin, 292.

Dobson, R.T. (2005), "Thermal modelling of a night sky radiation cooling system", *Journal of Energy in Southern Africa*, **16**, 2.

Ibrahim, K. (1993), "The Geological Frame Work for Harrat Ash-Shaam Basaltic, Super Group and Its Volcanotectonic Evolution," *Natural Resources Authority Bulletin*, **25**, 33.

Mallet, J.-L. (2002), "Geomodeling," Oxford University Press, New York. 624.

MWI (2000), "Ministry of Water and Irrigation. Outline hydrogeology of the Amman – Zarqa basin, Report," *Water Resources Policy Support*.13.

MWI (2010), Ministry of Water and Irrigation files and personal communications, Amman, Jordan.

Pollack, H.N., Hurter, S.J. and Johnson, J.R. (1993), " Heat flow from the earth's interior: analysis of the global data set," *Reviews of Geophysics* **31(3)**, 267-280.

Sass, J.H. Lachenbruch, A.H. and Monroe, R.J. (1971), "Thermal conductivity of rocks from measurements on fragments and its application to heat flow determinations," *J. Geophys. Res.* , **76**: 3391-3401.

Smadi, A. (2000), "The geology of Mafraq area," *Natural Resources Authority Bulletin*, **48**, 42.